PHYSICAL REVIEW A VOLUME 43, NUMBER 11 1 JUNE 1991

# Highly excited quasistable states of neutral CO lying up to the double-ionization-energy level

A. Dadouch, G. Dujardin, L. Hellner, and M. J. Besnard-Ramage
*Laboratoire de Photophysique Moléculaire, Bâtiment 213, Université de Paris–Sud, 91405 Orsay, France*
*and Laboratoire pour l'Utilisation du Rayonnement Electromagnétique,*
*Université de Paris–Sud, Bâtiment 209 D, 91405 Orsay, France*

B. J. Olsson
*Department of Physics I, Royal Institute of Technology, S-100 44 Stockholm, Sweden*

(Received 7 December 1990)

Highly excited states of neutral CO lying in the 20–40-eV excitation energy range, i.e., up to the double-ionization threshold energy, are studied by means of synchrotron radiation. They are observed as resonances in the ion-yield curves, which measure the $O^-$ and $C^-$ negative-fragment-ion intensity as a function of the photon excitation energy. Narrow resonances are assigned to doubly excited Rydberg-state series converging to $CO^+$ satellite states.

## I. INTRODUCTION

Doubly excited Rydberg states of atoms and molecules have attracted much attention[1,2] as valuable systems for studying electron-correlation effects. Furthermore, these highly excited electronic states can play an important role in other fields, such as near-resonant multiphoton single and multiple ionization or neutral and ion desorption from adsorbed molecules.[3]

Doubly excited Rydberg states of molecules in which one electron is promoted to an unfilled molecular orbital and a second electron is excited to a Rydberg orbital have been known to exist in the single-ionization-energy region, i.e., up to about 25 eV of excitation energy.[4] At higher energies, no resonances could be observed in the photoabsorption[5] or in the photoionization[6] spectra of simple diatomic molecules. It was then considered that at energies so high, molecular states would dissociate or autoionize so rapidly that they would not give rise to observable resonances.

The aim of this work is to demonstrate, by using the CO molecule as an example, that molecular resonances do exist in the 25–40-eV high-energy range, i.e., up to the double-ionization threshold energy [at 41.3 eV for CO (Ref. 7)]. Furthermore, some of these resonances have a narrow energy width (the measured width is limited by the experimental energy resolution). These high-energy resonances are detected by using the method previously used in the single-ionization[4,8,9] and core-ionization[10] energy regions. It consists in the detection of negative fragment ions issued from the predissociation of (doubly excited) Rydberg states by ion pair states:

$$AB + h\nu \rightarrow AB^{**} \rightarrow A^+ + B^- .$$

As compared to the photoionization and photoabsorption spectra, which are dominated by the ionization continua in the 25–40-eV energy range, the ion-pair formation is a much more sensitive probe of neutral states lying in this energy region. It will be shown in this paper that the detection of negative fragment ions is a powerful method to explore doubly excited Rydberg states lying between the single- and double-ionization threshold energies.

## II. EXPERIMENT

The synchrotron radiation from Super ACO (Orsay's storage ring) dispersed by a grazing incidence monochromator (450 lines/mm grating) is used as a photon source of variable energy in the 20–50-eV range.

The energy calibration is checked by using as references the three members of the Ar I $3s3p^6np$ series ($n=4,5,6$) near 440 Å (28 eV) (Ref. 11) and the three strong resonances near 270 Å (46 eV) of the Ne I $2s2p^6np$ ($n=3,4,5$) series.[12] Depending on the signal intensity the excitation bandpass is varied from 0.6 to 3 Å by changing the slit width of the monochromator.

Negative fragment ions are mass selected through a Riber SQX 156 quadrupole filter and counted as a function of the photon energy. These spectra are corrected for the variation of the photon excitation intensity as recorded from the photoemission of a gold mesh.

In order to ensure that detected negative ions are produced from unimolecular processes, the spectra are recorded at various gas pressures between $10^{-6}$ and $10^{-3}$ Torr. It is thus checked that the negative-ion signal is a linear function of the gas pressure and not a quadratic function, as would be the case if negative ions were produced by dissociative attachment on molecules of electrons being generated by photoionization of other molecules.

## III. RESULTS

The $O^-$ and $C^-$ ion-yield curves recorded in the 20–40-eV whole energy range of investigation are shown in Fig. 1.

The $O^-$ ion-yield curve is seen in more detail in Figs. 2 and 3. The corresponding resonance energies are listed in Tables I and II, respectively, and compared with those obtained by previous ion-pair[4] and photoabsorption[13] measurements. We note that no resonances could be detected beyond 23 eV in previous experiments,[4,13] whereas resonances are observed up to 39.9 eV in the present work. Furthermore, we see in Table I that our somewhat better energy resolution enables us to observe

TABLE I. Energies (in eV) of resonances observed in the $O^-$ yield curves of Fig. 2.

| Line No. in Fig. 2 | $O^-$ yield curve This work | $O^-$ yield curve Ref. 4 | Photoabsorption Ref. 13 |
|---|---|---|---|
| 1 | 20.98 | 20.94 | 20.936 |
| 2 | 21.02 | | |
| 3 | 21.07 | 21.07 | 21.068 |
| 4 | 21.13 | 21.13 | 21.126 |
| 5 | 21.20 | | |
| 6 | 21.25 | | 21.241 |
| 7 | 21.28 | 21.27 | |
| 8 | 21.33 | 21.31 | 21.313 |
| 9 | 21.40 | 21.42 | 21.416 |
| 10 | 21.44 | | 21.475 |
| 11 | 21.53 | 21.52 | 21.553 |
| 12 | 21.61 | 21.61 | 21.604 |
| 13 | 21.71 | 21.65 | 21.653 |
| 14 | 21.79 | 21.74 | 21.743 |
| 15 | 21.82 | 21.82 | 21.826 |
| 16 | 21.88 | 21.86 | |
| 17 | 21.97 | 21.93 | |
| 18 | 22.04 | 22.04 | 22.049 |
| 19 | 22.07 | 22.11 | 22.098 |
| 20 | 22.13 | 22.13 | |
| 21 | 22.18 | | 22.164 |
| 22 | 22.29 | 22.28 | 22.254 |
| 23 | 22.31 | | 22.327 |
| 24 | 22.40 | 22.40 | 22.390 |
| 25 | 22.44 | | |
| 26 | 22.50 | 22.50 | 22.495 |
| 27 | 22.56 | | 22.580 |
| 28 | 22.61 | 22.63 | |
| 29 | 22.73 | | |
| 30 | 22.78 | 22.80 | 22.828 |
| 31 | 22.90 | 22.93 | 22.915 |
| 32 | 22.96 | | 22.975 |
| 33 | 23.01 | | |
| 34 | 23.09 | | |
| 35 | 23.15 | | |
| 36 | 23.19 | 23.22 | |
| 37 | 23.27 | | |
| 38 | 23.34 | | |
| 39 | 23.40 | 23.38 | |
| 40 | 23.49 | | |
| 41 | 24.78 | | |
| 42 | 25.08 | | |
| 43 | 25.56 | | |
| 44 | 25.91 | | |
| 45 | 26.43 | | |
| 46 | 26.90 | | |
| 47 | 27.34 | | |
| 48 | 27.57 | | |
| 49 | 27.86 | | |
| 50 | 28.13 | | |

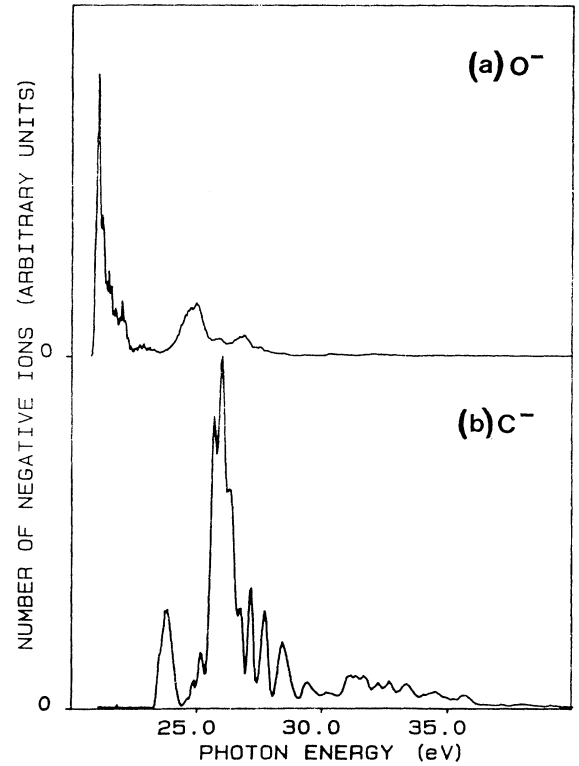

FIG. 1. (a) $O^-$ and (b) $C^-$ ion-yield curves recorded in the 20–40-eV photon energy range with instrumental bandwidths of about 1 and 3 Å, respectively.

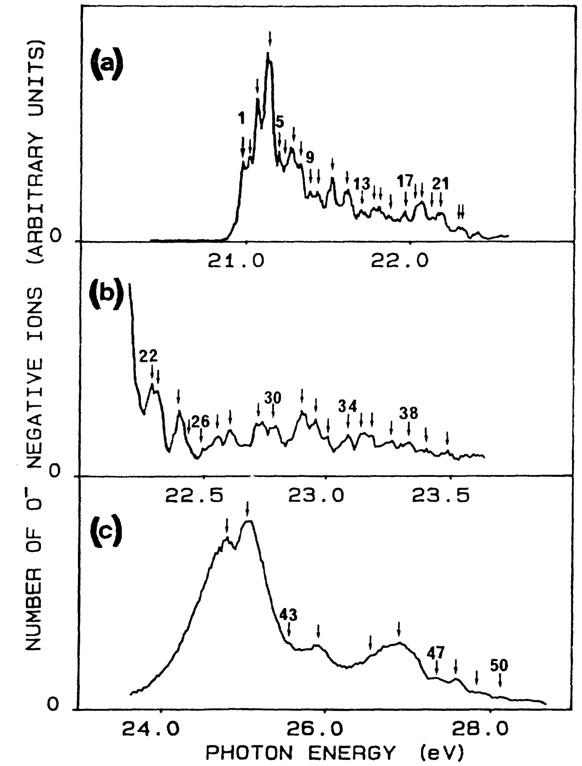

FIG. 2. $O^-$ ion-yield curves recorded with an instrumental bandwidth of about 1 Å ($\simeq$40 meV at 21 eV). Arrows with numbers indicate resonance energies of Table I.

more resonances in the 20.98–23.40-eV energy range than what was reported by Oertel, Schenk, and Baumgärtel.[4] The lowest energy for formation of $O^-$ ions is measured at 20.98 eV, which agrees well with the threshold energy for ion-pair formation,

$$CO + h\nu \rightarrow C^+(^2P) + O^-(^2P)$$

calculated[14] at 20.904 eV.

The $C^-$ ion-yield curve is shown in Fig. 4 with an enlarged energy scale. The resonance energies labeled in Fig. 4 are listed in Table III. No comparison with previous results is possible since no photoabsorption resonances could be observed in the 23.5–39-eV energy range.[13] Furthermore, Oertel, Schenk, and Baumgärtel[4] only detected a broad unresolved band in the 23–24.5-eV range. We note that the lowest resonance energy at 23.52 eV is quite compatible with the minimum energy of the ion-pair process

$$CO + h\nu \rightarrow C^-(^4S) + O^+(^4S)$$

calculated[4] at 23.45 eV.

We emphasize that the observed $O^-$ resonances generally do not coincide in energy with the $C^-$ ones. This is clearly seen in Fig. 5, which compares the $O^-$ and $C^-$ curves recorded at high-energy resolution under the same experimental conditions.

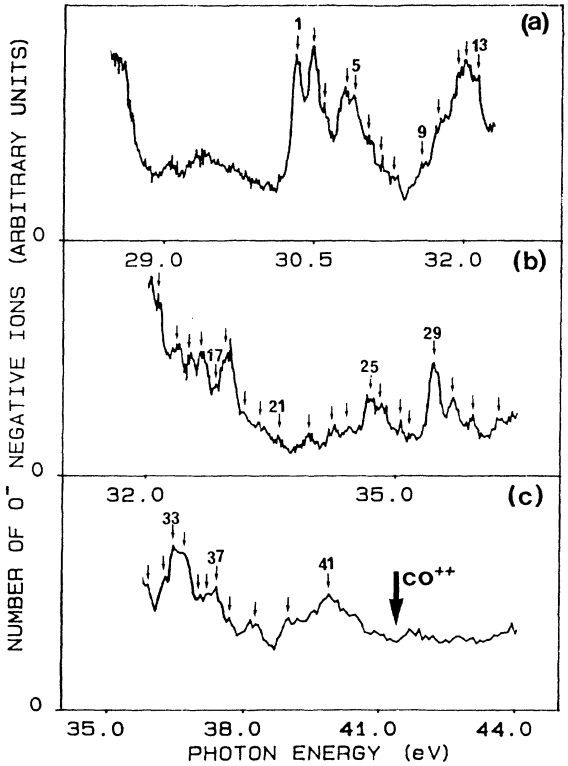

FIG. 3. $O^-$ ion-yield curves recorded with an instrumental bandwidth of (a) 0.8 Å, (b) 0.6 Å, and (c) 1 Å. Arrows with numbers indicate resonance energies of Table II.

TABLE II. Energies (in eV) of the resonances observed in the $O^-$ yield curves of Fig. 3.

| Line No. in Fig. 3 | $O^-$ yield curve This work | Line No. in Fig. 3 | $O^-$ yield curve This work |
|---|---|---|---|
| 1 | 30.33 | 21 | 33.62 |
| 2 | 30.50 | 22 | 33.96 |
| 3 | 30.61 | 23 | 34.26 |
| 4 | 30.83 | 24 | 34.44 |
| 5 | 30.90 | 25 | 34.69 |
| 6 | 31.08 | 26 | 34.83 |
| 7 | 31.19 | 27 | 35.06 |
| 8 | 31.31 | 28 | 35.20 |
| 9 | 31.58 | 29 | 35.46 |
| 10 | 31.76 | 30 | 35.69 |
| 11 | 31.95 | 31 | 35.89 |
| 12 | 32.04 | 32 | 36.25 |
| 13 | 32.15 | 33 | 36.42 |
| 14 | 32.35 | 34 | 36.70 |
| 15 | 32.53 | 35 | 37.20 |
| 16 | 32.67 | 36 | 37.38 |
| 17 | 32.83 | 37 | 37.51 |
| 18 | 32.95 | 38 | 37.66 |
| 19 | 33.15 | 39 | 38.21 |
| 20 | 33.37 | 40 | 38.99 |
|  |  | 41 | 39.90 |

TABLE III. Energies (in eV) of the resonances observed in the $C^-$ yield curves of Fig. 4.

| Line No. in Fig. 4 | $C^-$ yield curve This work | Line No. in Fig. 4 | $C^-$ curve This work |
|---|---|---|---|
| 1 | 23.52 | 27 | 29.44 |
| 2 | 23.57 | 28 | 30.18 |
| 3 | 23.63 | 29 | 30.36 |
| 4 | 23.71 | 30 | 30.65 |
| 5 | 23.73 | 31 | 30.83 |
| 6 | 23.77 | 32 | 31.08 |
| 7 | 23.84 | 33 | 31.38 |
| 8 | 23.88 | 34 | 31.71 |
| 9 | 23.94 | 35 | 32.17 |
| 10 | 23.98 | 36 | 32.28 |
| 11 | 24.01 | 37 | 32.67 |
| 12 | 24.03 | 38 | 32.93 |
| 13 | 24.10 | 39 | 33.37 |
| 14 | 24.15 | 40 | 33.57 |
| 15 | 24.23 | 41 | 33.88 |
| 16 | 24.27 | 42 | 34.14 |
| 17 | 24.70 | 43 | 34.41 |
| 18 | 24.92 | 44 | 34.58 |
| 19 | 25.25 | 45 | 34.90 |
| 20 | 25.73 | 46 | 35.11 |
| 21 | 26.05 | 47 | 35.46 |
| 22 | 26.40 | 48 | 35.72 |
| 23 | 26.80 | 49 | 36.09 |
| 24 | 27.21 | 50 | 36.48 |
| 25 | 27.77 | 51 | 37.13 |
| 26 | 28.47 | 52 | 38.08 |
|  |  | 53 | 39.06 |

From the examination of the curves in Figs. 2–4, we remark that three distinct energy regions can be distinguished. Between 20.9 and 24 eV, $O^-$ and $C^-$ resonances are rather narrow and some of them have a width that is limited by the experimental resolution. For example, the 50-meV width of resonance number 4 in Fig. 2 is certainly limited by the 40-meV instrumental bandpass. The 24–30-eV energy range is characterized by very broad resonances both in the $O^-$ and $C^-$ curves. The 30–40-eV energy interval again shows narrow resonances.

The width of some resonances is larger than the instrumental bandpass. This may be due to one of the following reasons: (i) the overlap of unresolved resonances, (ii) the natural bandwidth related to a very fast predissociation, (iii) the Franck-Condon width of directly populated dissociative ion-pair states, (iv) the rotational envelop of the vibronic bands. Higher-energy resolution experiments performed with rotationally cooled molecules in a supersonic beam would be needed in order to clarify this problem.

## IV. DISCUSSION

The electronic configuration of carbon monoxide in its $X\,^1\Sigma^+$ ground state is[15]

$$(1\sigma)^2(2\sigma)^2(3\sigma)^2(4\sigma)^2(1\pi)^4(5\sigma)^2(2\pi)^0(6\sigma^0) .$$

The removal of one electron from the $5\sigma$, $1\pi$, $4\sigma$, and $3\sigma$ orbitals gives rise to electronic states of the $CO^+$ ion with ionization energies of 14.01, 16.54, 19.67, and 38.3 eV, respectively.[15,16] It follows that most of the observed resonances in the $O^-$ and $C^-$ ion-yield curves lying in the 21–39-eV energy range cannot be ascribed to singly excited valence or Rydberg states of the CO molecule. We will then attempt in the following to assign these resonances to doubly excited Rydberg states which may be populated by excitation of two electrons, one electron being excited to an unoccupied valence orbital and a second electron being excited to a Rydberg orbital. Energies of the resonances ($E^{v,\lambda}_{\rm mol}$, where $v$ is the vibrational level and $\lambda$ is the electronic state of CO) are related to the energies of the ionic states ($E^{v,\lambda'}_{\rm ion}$, where $v$ is the vibrational level and $\lambda'$ is the electronic state of $CO^+$) via the Rydberg formula:

$$E^{v,\lambda}_{\rm mol}=E^{v,\lambda'}_{\rm ion}-\frac{\mathcal{R}}{(n-\delta)^2} ,$$

where $\mathcal{R}$, $n$, and $\delta$ are the Rydberg constant, the principal quantum number, and the quantum defect, respectively. It is then essential, before discussing the assignment of CO resonances, to summarize what is known on the energies and the electronic configurations of the $CO^+$ ionic states.

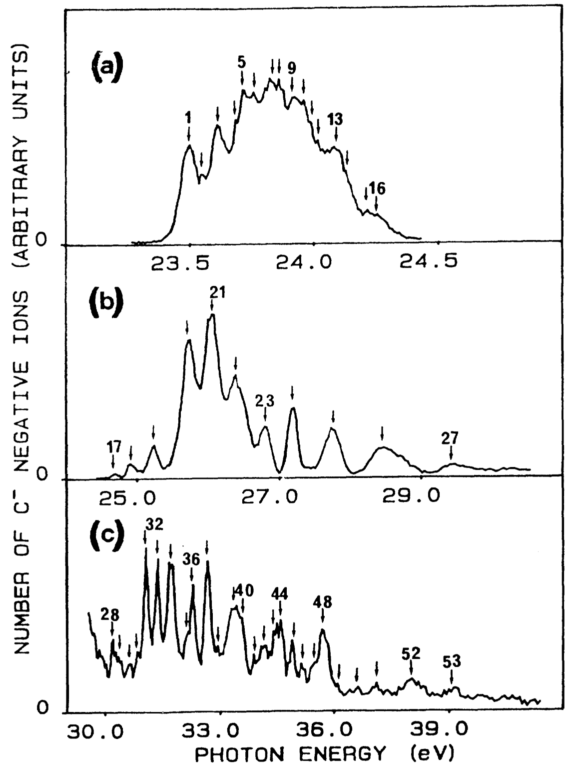

FIG. 4. $C^-$ ion-yield curves recorded with an instrumental bandwidth of 1 Å. Arrows with numbers indicate resonance energies of Table III.

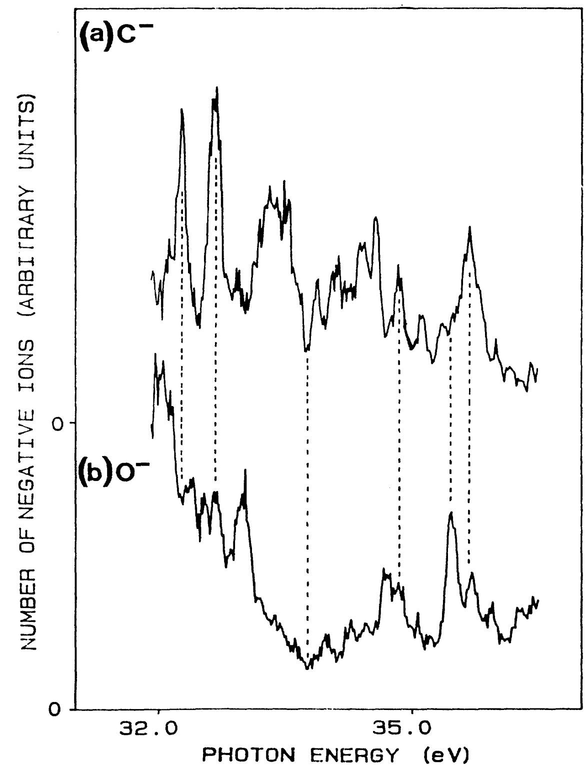

FIG. 5. Comparison of $C^-$ and $O^-$ ion-yield curves recorded with an instrumental bandwidth of 0.6 Å.

TABLE IV. Vertical energies and dominant electronic configurations of $CO^+$ electronic states.

| Electronic state | Vertical energy (eV) | Occupation number of molecular orbitals of CO KK | $3\sigma$ | $4\sigma$ | $1\pi$ | $5\sigma$ | $2\pi$ | $6\sigma$ | Ref. |
|---|---|---|---|---|---|---|---|---|---|
| $CO(X\,^1\Sigma^+)$ | 0[a] | | 2 | 2 | 4 | 2 | 0 | 0 | 18,20 |
| $CO^+(X\,^2\Sigma^+)$ | 14.014[a] | | 2 | 2 | 4 | 1 | 0 | 0 | 18,20 |
| $CO^+(A\,^2\Pi)$ | 16.585[a] | | 2 | 2 | 3 | 2 | 0 | 0 | 15 |
| $CO^+(B\,^2\Sigma^+)$ | 19.702[a] | | 2 | 1 | 4 | 2 | 0 | 0 | 18,20 |
| $CO^+(C\,^2\Delta)$ | 21.827[b] | | 2 | 2 | 3 | 1 | 1 | 0 | 24,26 |
| $CO^+(D\,^2\Pi)$ | 22.734[c] | | 2 | 2 | 2 | 2 | 1 | 0 | 21 |
| $CO^+(E\,^2\Sigma^+)$ | 23.383[c] | | 2 | 2 | 3 | 1 | 1 | 0 | 18,20,21 |
| $CO^+(E'\,^2\Sigma^+)$ | 25.483[c] | | 2 | 2 | 3 | 1 | 1 | 0 | 18,20,21 |
| $CO^+(F\,^2\Sigma^+)$ | 27.44[d] | | 2 | 2 | 4 | 0 | 0 | 1 | 18,20 |
| $CO^+(G\,^2\Sigma^+)$ | 28.086[c] | | 2 | 1 | 3 | 2 | 1 | 0 | 18 |
| | 31.8[e] | | | | | | | | |
| | 33.7[e] | | | | | | | | |
| | 36.3[e] | | | | | | | | |
| $CO^+(^2\Sigma^+3\sigma^{-1})$ | 38.3[f] | | 1 | 2 | 4 | 2 | 0 | 0 | 18 |

[a] Reference 25.
[b] Reference 24 and 26.
[c] Reference 21.
[d] Reference 22.
[e] Reference 16.
[f] Reference 15.

### A. Energies and electronic configurations of the $CO^+$ ionic states

Numerous theoretical[17–20] and experimental photoelectron spectroscopic[15,16,21–23] works have been devoted to the $CO^+$ electronic state studies. However, despite this large effort, a satisfactory description of the highly excited electronic states of $CO^+$ is still an unsolved problem. Data from the literature are collected in Table IV. There are four $CO^+$ electronic states [$X\,^2\Sigma^+$, $A\,^2\Pi$, $B\,^2\Sigma^+$, and $^2\Sigma^+$ $(3\sigma^{-1})$] whose dominant electronic configuration is a monoexcited configuration with respect to that of CO in its electronic ground state. These states are rather well characterized.[15,24] The $CO^+(C\,^2\Delta)$ state could be observed only by optical emission spectroscopy.[25] This emission was recently reinvestigated in more detail by Cossart and Cossart-Magos.[26] This state could not be observed by photoelectron spectroscopy most probably because of a very different geometry as compared to the CO ground state.[26] The $CO^+(D\,^2\Pi$, $E\,^2\Sigma^+$, $E'\,^2\Sigma^+$, and $G\,^2\Sigma^+)$ states were observed with their vibrational structures in the high-resolution photoelectron study of Asbrink *et al.*[21] The dominant electronic configurations listed in Table IV were chosen from those proposed in the literature[18,20,21] by assuming that the most favorable configurations have only two electrons excited and involve only those molecular CO orbitals (up to $6\sigma$) that are built from occupied atomic orbitals.[15] The $CO^+(F\,^2\Sigma^+)$ state was observed in the photoelectron spectra of Asbrink *et al.*[21] However, these authors assigned the corresponding features to an impurity line in the helium light source. A recent[22] investigation using synchrotron radiation as a photon source confirmed the observation of these bands in the 27.0–27.5-eV ionization energy range. This establishes the existence of a new $CO^+(F\,^2\Sigma^+)$ electronic state. The most difficult ioniza-

TABLE V. Energies $E$ (eV) (from Table I) and effective quantum numbers $n^*=n-\delta$ of Rydberg series converging to the $D\,^2\Pi$ state of $CO^+$. The $CO^+$ level energies are taken from Ref. 21.

| Vibrational level $V$ | *np* CO Rydberg progressions 4*p* Mean $n^*=3.31$ $E$ (eV) | $n^*$ | 5*p* Mean $n^*=4.33$ $E$ (eV) | $n^*$ | 6*p* Mean $n^*=5.24$ $E$ (eV) | $n^*$ | 7*p* Mean $n^*=6.35$ $E$ (eV) | $n^*$ | $CO^+$ state $D^2\Pi$ $E$ (eV)[a] |
|---|---|---|---|---|---|---|---|---|---|
| 0 | | | 21.33 | 4.39 | 21.53 | 5.15 | 21.71 | 6.42 | 22.039 |
| 1 | 20.98 | 3.29 | 21.53 | 4.38 | | | 21.88 | 6.20 | 22.234 |
| 2 | 21.13 | 3.28 | | | | | 22.07 | 6.40 | 22.402 |
| 3 | 21.33 | 3.32 | 21.82 | 4.26 | 22.07 | 5.24 | | | 22.565 |
| 4 | 21.53 | 3.30 | | | | | 22.40 | 6.39 | 22.734 |
| 5 | | | 22.18 | 4.39 | 22.44 | 5.40 | 22.56 | 6.29 | 22.904 |
| 6 | 21.82 | 3.30 | 22.31 | 4.25 | 22.56 | 5.20 | 22.73 | 6.35 | 23.064 |
| 7 | 21.97 | 3.28 | 22.50 | 4.31 | 22.73 | 5.20 | 22.90 | 6.41 | 23.230 |

[a] Reference 21.

tion energy region to study both experimentally and theoretically is the 30–38-eV range. One guesses from the results of Krummacher *et al.*[16] that several $CO^+$ electronic states (including the three states whose ionization energies at 31.8, 33.7, and 36.2 eV are mentioned in Table IV) lie in this energy range. However, no clear identification of these electronic states can be made.

### B. Resonances in the 20.9–24-eV energy range

Resonances in the 20.9–24-eV energy range are assigned to doubly excited Rydberg state series converging to the $D\,^2\Pi$, $E\,^2\Sigma^+$, and $E'\,^2\Sigma^+$ states of $CO^+$. Our assignment of the resonances observed in the $O^-$ and $C^-$ ion-yield curves is shown in Tables V–VII. It differs somewhat from that of Asbrink *et al.*[21] and Codling and Potts,[13] who previously assigned the photoabsorption resonances. In the present work, more Rydberg series and longer vibrational progressions could be observed as compared to the photoabsorption study.[21] We note that, in our assignment, a given resonance may belong to various Rydberg series. This is due to the possible overlap of several resonances within our instrumental resolution. Rydberg series are identified by comparing the quantum defects with those of the singly excited Rydberg series of CO that have been analyzed by Lefebvre-Brion, Moser, and Nesbet[27] and Lindholm.[28]

Table VIII shows the comparison between quantum defects of doubly excited Rydberg states (this work) and those of singly excited Rydberg states.[28] There seems to be an unambiguous correspondance between quantum defects of doubly excited Rydberg states and those of singly excited Rydberg states.

### C. Resonances in the 24–30-eV energy range

In the 24–30-eV energy range, only broad resonances are observed in both the $O^-$ (Fig. 2) and $C^-$ (Fig. 4) ion-yield curves. The widths of these bands are not limited by instrumental resolution and seem not to be only due to the overlapping of unresolved bands. The observed widths are then believed to be related to the real widths of these levels. Rydberg states of CO in this energy range would belong to series converging to the $F\,^2\Sigma^+$ and $G\,^2\Sigma^+$ of $CO^+$ (see Table IV). These latter states are known to have quasistable vibrational levels in the Franck-Condon region since they give rise to well-resolved vibrational progressions in the photoelectron spectra.[21,22] Assignment of the broad resonances of Figs. 2 and 4 to Rydberg states would then require that a very rapid predissociation by CO ion-pair states greatly enlarge the widths of these levels. An alternative explanation would assign these broad resonances to direct transitions to the repulsive part of ion-pair states.

TABLE VI. Energies $E$ (eV) and effective quantum numbers $n^*=n-\delta$ of Rydberg series converging to the $E\,^2\Sigma^+$ state of $CO^+$. The $CO^+$ level energies are taken from Ref. 21. Energies that are underlined are those from the $C^-$ ion-yield curve (Table III). Other energies are from the $O^-$ ion-yield curve (Table I).

| | *nsσ* CO Rydberg progression | | | | | | | | |
|---|---|---|---|---|---|---|---|---|---|
| Vibrational level | 4*sσ* | | 5*sσ* | | 6*sσ* | | 7*sσ* | | $CO^+$ state |
| | Mean $n^*=3.09$ | | Mean $n^*=4.08$ | | Mean $n^*=5.01$ | | Mean $n^*=6.11$ | | $E\,^2\Sigma^+$ |
| $V$ | $E$ (eV) | $n^*$ | $E$ (eV) | $n^*$ | $E$ (eV) | $n^*$ | $E$ (eV) | $n^*$ | $E$ (eV)[a] |
| 0 | 21.61 | 3.09 | 22.18 | 4.02 | 22.50 | 5.01 | | | 23.039 |
| 1 | 21.79 | 3.09 | 22.40 | 4.10 | | | | | 23.212 |
| 2 | 21.97 | 3.10 | 22.56 | 4.07 | | | 23.01 | 6.03 | 23.383 |
| 3 | 22.13 | 3.09 | 22.73 | 4.04 | 23.01 | 4.97 | 23.19 | 6.11 | 23.559 |
| 4 | 22.31 | 3.10 | 22.90 | 4.04 | 23.19 | 5.03 | | | 23.732 |
| 5 | 22.44 | 3.07 | 23.09 | 4.17 | 23.34 | 5.03 | 23.52 | 5.18 | 23.874 |
| 6 | 22.56 | 3.08 | 23.19 | 4.12 | | | 23.63 | 6.11 | 23.994 |

| | *npσ*, *npπ*, and *np* CO Rydberg progressions | | | | | | | | | | |
|---|---|---|---|---|---|---|---|---|---|---|---|
| Vibrational level | 3*pσ* | | 3*pπ* | | 4*p* | | 5*p* | | 6*p* | | $CO^+$ state |
| | Mean $n^*=2.29$ | | Mean $n^*=2.34$ | | Mean $n^*=3.35$ | | Mean $n^*=4.34$ | | Mean $n^*=5.34$ | | $E\,^2\Sigma^+$ |
| $V$ | $E$ (eV) | $n^*$ | $E$ (eV) | $n^*$ | $E$ (eV) | $n^*$ | $E$ (eV) | $n^*$ | $E$ (eV) | $n^*$ | $E$ (eV)[a] |
| 0 | | | | | 21.82 | 3.34 | 22.31 | 4.33 | 22.56 | 5.33 | 23.039 |
| 1 | | | | | 21.97 | 3.31 | 22.50 | 4.36 | 22.73 | 5.30 | 23.212 |
| 2 | | | | | 22.13 | 3.30 | | | 22.90 | 5.30 | 23.383 |
| 3 | 20.98 | 2.30 | 21.07 | 2.34 | 22.31 | 3.30 | | | 23.09 | 5.39 | 23.559 |
| 4 | 21.13 | 2.29 | 21.25 | 2.34 | 22.56 | 3.41 | 23.01 | 4.34 | 23.27 | 5.42 | 23.732 |
| 5 | 21.28 | 2.29 | 21.40 | 2.34 | | | 23.15 | 4.34 | 23.40 | 5.38 | 23.874 |
| 6 | 21.38 | 2.29 | 21.53 | 2.35 | 22.78 | 3.35 | 23.27 | 4.33 | 23.52 | 5.34 | 23.994 |

[a] Reference 21.

### D. Resonances in the 30–40-eV energy range

Resonances are observed in the $O^-$ (Fig. 3) and $C^-$ (Fig. 4) ion-yield curves up to the double photoionization threshold energy at 41.3 eV.[10] Contrary to the case discussed in Sec. IV C, resonances in the 30–40-eV energy range are narrow and some of them have a width limited by the instrumental resolution. Although these resonances are believed to correspond to CO Rydberg-state series converging to the $CO^+$ electronic states lying in the 31–38-eV range, no assignment can be achieved at the present time. This is mainly due to the lack of data on the $CO^+$ electronic states. As discussed in Sec. IV A, satellite states of $CO^+$ in this high-energy region are very poorly known. From the present observation of narrow resonances, we can conclude that the $CO^+$ electronic states to which these Rydberg series converge may also have well-resolved vibrational structures. This is then an encouragement for future photoelectron studies of these states. A careful look at the curves of Fig. 3 indicates that the resonances are clustered into several groups of which the energy limits are the following: 30–31.5, 31.5–33.8, 33.8–35.2, and 35.2–38.2 eV. These four groups may well correspond to Rydberg series converging to four separate $CO^+$ electronic states. However, any confirmation and more precise assignment have to wait for further photoelectron data.

## V. CONCLUSION

Highly excited states (up to the double ionization energy) of neutral CO have been shown to be stable enough to give rise to vibronic resonances in the $O^-$ and $C^-$ ion-yield curves. Similar observations have been made with other diatomic molecules like $O_2$ and NO.[29] The photoelectron data of $N_2$ (Ref. 30) also reveal some discrete structures in $N_2{}^+$ between 30 and 40 eV. This suggests that highly excited states of the neutral $N_2$ molecule probably exist in this energy range as Rydberg-state series converging to these $N_2{}^+$ states. However, the negative-fragment-ion detection method cannot be used in this case since $N^-$ ions are not stable.

TABLE VII. Energies $E$ (eV) and effective quantum numbers $n^* = n - \delta$ of Rydberg series converging to the $E'\,^2\Sigma^+$ state of $CO^+$. The $CO^+$ level energies are taken from Ref. 21. Energies that are underlined are those from the $C^-$ ion-yield curve (Table III). Other energies are from the $O^-$ ion-yield curve (Table I).

| Vibrational levels $V$ | $ns\sigma$ CO Rydberg progressions<br>$3s\sigma$ Mean $n^*=1.98$<br>$E$ (eV) | $n^*$ | $4s\sigma$ Mean $n^*=2.95$<br>$E$ (eV) | $n^*$ | $5s\sigma$ Mean $n^*=4.02$<br>$E$ (eV) | $n^*$ | $CO^+$ state $E'\,^2\Sigma^+$ $E$ (eV)[a] |
|---|---|---|---|---|---|---|---|
| 0 | 21.28 | 1.98 | 23.19 | 2.94 | 23.94 | 4.05 | 24.770 |
| 1 | 21.44 | 1.97 | 23.40 | 2.97 | 24.10 | 4.01 | 24.942 |
| 2 | 21.61 | 1.97 | 23.57 | 2.96 | 24.27 | 4.01 | 25.118 |
| 3 | 21.82 | 1.98 | 23.73 | 2.94 | | | 25.303 |
| 4 | 22.04 | 1.99 | 23.94 | 2.97 | | | 25.483 |
| 5 | 22.18 | 1.98 | 24.10 | 2.94 | | | 25.667 |
| 6 | 22.40 | 1.99 | 24.27 | 2.94 | | | 25.842 |
| 7 | 22.56 | 1.99 | | | | | 26.012 |
| 8 | 22.73 | 1.98 | | | | | 26.180 |
| 9 | 22.90 | 1.98 | | | | | 26.371 |
| 10 | 23.09 | 1.99 | | | | | 26.534 |

| Vibrational levels $V$ | $np\sigma$, $np\pi$, and $np$ CO Rydberg progressions<br>$3p\sigma$ Mean $n^*=2.28$<br>$E$ (eV) | $n^*$ | $3p\pi$ Mean $N^*=2.36$<br>$E$ (eV) | $n^*$ | $4p$ Mean $n^*=3.30$<br>$E$ (eV) | $n^*$ | $5p$ Mean $n^*=4.29$<br>$E$ (eV) | $n^*$ | $CO^+$ state $E'\,^2\Sigma^+$ $E$ (eV)[a] |
|---|---|---|---|---|---|---|---|---|---|
| 0 | 22.13 | 2.27 | 22.29 | 2.34 | 23.52 | 3.30 | 24.03 | 4.29 | 24.770 |
| 1 | 22.31 | 2.27 | 22.50 | 2.36 | 23.71 | 3.32 | 24.23 | 4.37 | 24.942 |
| 2 | 22.50 | 2.28 | | | 23.88 | 3.31 | | | 25.118 |
| 3 | 22.73 | 2.30 | | | 24.03 | 3.27 | | | 25.303 |
| 4 | 22.90 | 2.29 | 23.10 | 2.35 | 24.23 | 3.30 | 24.78 | 4.38 | 25.483 |
| 5 | | | 23.19 | 2.35 | | | 24.92 | 4.26 | 25.667 |
| 6 | 23.19 | 2.27 | 23.40 | 2.36 | | | 25.08 | 4.22 | 25.842 |
| 7 | 23.40 | 2.28 | 23.57 | 2.36 | 24.78 | 3.32 | 25.25 | 4.22 | 26.012 |
| 8 | 23.57 | 2.28 | 23.71 | 2.35 | 24.92 | 3.28 | | | 26.180 |
| 9 | 23.77 | 2.29 | 23.94 | 2.37 | | | | | 26.371 |
| 10 | 23.94 | 2.29 | 24.10 | 2.36 | | | | | 26.534 |

[a] Reference 21.

Some of the CO resonances are tentatively assigned to doubly excited Rydberg series converging to the $D\,^2\Pi$, $E\,^2\Sigma^+$, and $E'\,^2\Sigma^+$ satellite states of $CO^+$. Rydberg states with higher energies could not be analyzed because of the lack of data on the highly excited satellite $CO^+$ states lying above 30 eV. High-resolution photoelectron spectroscopy experiments are then much needed.

We emphasize that no evidence of the known shape resonances in CO (Refs. 31–33) could be obtained in this work, although a coupling between shape resonances and

TABLE VIII. Comparison of doubly excited Rydberg state and singly excited Rydberg-state quantum defects ($\delta$).

| | $\delta$ | |
|---|---|---|
| *nl* | Doubly excited Rydberg series converging to the $D\,^2\Pi$ state of $CO^+$ $1\pi,1\pi\rightarrow 2\pi,nl$ (This work) | Singly excited Rydberg series converging to the $X\,^2\Sigma^+$ state of $CO^+$ $1\pi\rightarrow nl$ (Ref. 28) |
| 4*p* | 0.69 | |
| 5*p* | 0.67 | $(np\sigma)$ 0.72, $(np\pi)$ 0.65 |
| 6*p* | 0.76 | |
| 7*p* | 0.65 | |

| | $\delta$ | |
|---|---|---|
| *nl* | Doubly excited Rydberg series converging to the $E\,^2\Sigma^+$ state of $CO^+$ $1\pi,5\sigma\rightarrow 2\pi,nl$ (This work) | Singly excited Rydberg series converging to the $X\,^2\Sigma^+$ state of $CO^+$ (Ref. 28) |
| 4*s* | 0.91 | |
| 5*s* | 0.92 | $5\sigma\rightarrow nl$, $(ms\sigma)$ 0.90 |
| 6*s* | 0.99 | |
| 7*s* | 0.89 | |
| $3p\sigma$ | 0.71 | |
| $3p\pi$ | 0.66 | $1\pi\rightarrow nl$, $(np\sigma)$ 0.72, $(np\pi)$ 0.65 |
| 4*p* | 0.65 | |
| 5*p* | 0.66 | |
| 6*p* | 0.65 | |

| | $\delta$ | |
|---|---|---|
| *nl* | Doubly excited Rydberg series converging to the $E'\,^2\Sigma^2$ state of $CO^+$ $1\pi,5\sigma\rightarrow 2\pi,nl$ (This work) | Singly excited Rydberg series converging to the $X\,^2\Sigma^+$ state of $CO^+$ $1\pi\rightarrow nl$ (Ref. 28) |
| 3*s* | 1.02 | |
| 4*s* | 1.05 | $(ms\sigma)$ 1.04 |
| 5*s* | 0.98 | |
| $3p\sigma$ | 0.72 | |
| $3p\pi$ | 0.64 | $(np\sigma)$ 0.72, $(np\pi)$ 0.65 |
| 4*p* | 0.70 | |
| 5*p* | 0.71 | |

ion-pair states may be expected to exist. This was indeed recently observed in $O_2$.[29]

Ion-pair formation and the subsequent detection of negative fragment ions have proven to be a very powerful probe of highly excited CO states lying in the 20–40-eV energy range. However, numerous other relaxation pathways such as emission of fluorescence, autoionization,[34] or predissociation into excited neutral fragments may compete with ion-pair formation. In particular, the autoionization channels could be important as such high internal energies.

Much further work is necessary to unambiguously assing the observed highly excited resonances and to explore their various relaxation channels.

## ACKNOWLEDGMENTS

We thank Dr. H. Lefebvre-Brion for helpful discussions and Professor J. Comer for communicating his results prior to publication.

---

[1] P. R. Woodruff and J. A. R. Samson, Phys. Rev. A **25**, 848 (1982).
[2] C. Bordas, J. L. Vialle, and M. Broyer, Phys. Rev. Lett. **64**, 1223 (1990).
[3] D. E. Ramaker, J. Chem. Phys. **78**, 2998 (1982).
[4] H. Oertel, H. Schenk, and H. Baumgärtel, Chem. Phys. **46**, 251 (1980).
[5] L. C. Lee, R. W. Carlson, D. L. Judge, and M. Ogawa, J. Quant. Spectrosc. Radiat. Transfer **13**, 1023 (1973).
[6] T. Masuoka, J. Chem. Phys. **82**, 3921 (1985).
[7] D. Dujardin, L. Hellner, M. Hamdan, A. G. Brenton, B. J. Olsson, and M. J. Besnard-Ramage, J. Phys. B **23**, 1165 (1990).
[8] A. J. Yencha, D. K. Kela, R. J. Donovan, A. Hopkirk, and A. Kvaran, Chem. Phys. Lett. **165**, 283 (1990).
[9] K. Mitsuke, S. Suzuki, T. Imamura, and I. Koyano, J. Chem. Phys. **93**, 1710 (1990).
[10] G. Dujardin, L. Hellner, B. J. Olsson, M. J. Besnard-Ramage, and A. Dadouch, Phys. Rev. Lett. **62**, 745 (1989).
[11] R. P. Madden, D. L. Ederer, and K. Codling, Phys. Rev. **177**, 136 (1969).
[12] K. Codling, R. P. Madden, and D. L. Ederer, Phys. Rev. **155**, 26 (1967).
[13] K. Codling and A. W. Potts, J. Phys. B **7**, 163 (1974).
[14] R. Locht and J. M. Dürer, Chem. Phys. Lett. **34**, 508 (1975).
[15] K. Siegbahn, C. Nordling, G. Johansson, J. Hedman, P. F. Heden, K. Hamrin, U. Gelius, T. Bergmark, L. O. Werme, R. Manne, and Y. Baer, *ESCA Applied to Free Molecules* (North-Holland, Amsterdam, 1969).
[16] S. Krummacher, V. Schmidt, F. Wuillemier, J. M. Bizau, and D. Ederer, J. Phys. B **16**, 1733 (1983).
[17] M. Okuda and N. Jonathan, J. Electron Spectrosc. Relat. Phenom. **3**, 19 (1974).
[18] P. S. Bagus and E. K. Viinikka, Phys. Rev. A **15**, 1486 (1977).
[19] J. Schirmer, L. S. Cederbaum, W. Domcke, and W. Von Niessen, Chem. Phys. **26**, 149 (1977).
[20] P. W. Langhoff, S. R. Langhoff, T. N. Rescigno, J. Schirmer, L. S. Cederbaum, W. Domcke, and W. Von Niessen, Chem. Phys. **58**, 71 (1981).
[21] L. Asbrink, C. Fridh, E. Lindholm, and K. Codling, Physica Scr. **10**, 183 (1974).
[22] J. Comer (private communication).
[23] J. L. Gardner and J. A. R. Samson, J. Chem. Phys. **62**, 1447 (1975).
[24] K. P. Huber and G. Herzberg, *Constants of Diatomic Molecules* (Van Nostrand-Reinhold, New York, 1979).
[25] J. Marchant, J. D'Incan, and J. Janin, Spectrochim Acta, Part A **25** 605 (1969).
[26] D. Cossart and C. Cossart-Magos, J. Mol. Spectrosc. **141**, 59 (1990).
[27] H. Lefebvre-Brion, C. M. Moser, and R. K. Nesbet, J. Mol. Spectrosc. **13**, 418 (1964).
[28] E. Lindholm, Ark. Fys. **40**, 103 (1968).
[29] A. Dadouch, G. Dujardin, L. Hellner, M. J. Besnard-Ramage, and B. Olsson (unpublished).
[30] S. Krummacher, V. Schmidt, and F. Wuillemier, J. Phys. B **13**, 3993 (1980).
[31] R. Stockbauer, B. E. Cole, D. L. Ederer, J. B. West, A. C. Parr, and J. L. Dehmer, Phys. Rev. Lett. **43**, 757 (1979).
[32] K. Ito, A. Tabché-Fouhaité, H. Frohlich, P. M. Guyon, and I. Nenner, J. Chem. Phys. **82**, 1231 (1985).
[33] N. Padial, G. Csanak, B. V. McKoy, and P. W. Langhoff, J. Chem. Phys. **69** 2992 (1978).
[34] L. Karlsson, S. Svensson, and A. Svensson, J. Phys. B **22**, 3423 (1989).